HHS Public Access

Author manuscript

Genes Chromosomes Cancer. Author manuscript; available in PMC 2023 May 31.

Published in final edited form as:

Genes Chromosomes Cancer. 2023 January ; 62(1): 5–16. doi:10.1002/gcc.23082.

RREB1::MRTFB Fusion Positive Extra-glossal Mesenchymal Neoplasms: A Series of Five Cases Expanding Their Anatomic Distribution And Highlighting Significant Morphological and Phenotypic Diversity

Abbas Agaimy, MD[1], **Nasir Ud Din, MBBS**[2], **Josephine K. Dermawan, MD, PhD**[3], **Florian Haller, MD**[1], **Katja Melzer, MD**[4], **Axel Denz, MD**[5], **Daniel Baumhoer, MD**[6], **Robert Stoehr, PhD**[1], **Robert Grützmann, MD**[5], **Cristina R. Antonescu, MD**[3]

[1]Institute of Pathology, Friedrich Alexander University Erlangen-Nürnberg, University Hospital, Erlangen, Germany

[2]Department of Pathology and Laboratory Medicine, Aga Khan University, Karachi, Pakistan

[3]Department of Pathology, Memorial Sloan-Kettering Cancer Center, New York, NY

[4]Institute of Radiology, Friedrich Alexander University Erlangen-Nürnberg, University Hospital, Erlangen, Germany

[5]Department of Surgery, Friedrich Alexander University Erlangen-Nürnberg, University Hospital, Erlangen, Germany

[6]Institute of Pathology, University Hospital Basel, University of Basel, Basel, Switzerland

Abstract

The *RREB1::MRTFB* (former *RREB1::MKL2)* fusion characterizes ectomesenchymal chondromyxoid tumors of the tongue (EMCMT). Only five molecularly confirmed extra-glossal EMCMT cases have been reported recently; all occurring at head and neck or mediastinal sites. We herein describe five new cases including the first two extracranial/extrathoracic cases. The tumors occurred in three male and two female patients with an age ranging from 18 to 61 years (median, 28). Three tumors were located in the head and neck (jaw, parapharyngeal space and nasopharyngeal wall) and two in the soft tissue (inguinal and presacral). The tumor size ranged from 3.3 to 20 cm (median, 7). Treatment was surgical without adjuvant treatment in all cases. Two cases were disease-free at 5 and 17 months; other cases were lost to follow-up. Histologically, the soft tissue cases shared a predominant fibromyxoid appearance, but with variable cyto-architectural pattern (cellular perineurioma-like whorls and storiform pattern in one case and large polygonal granular cells embedded within a chondromyxoid stroma in the other). Two tumors (inguinal and parapharyngeal) showed spindled to ovoid and round cells with a moderately to highly cellular nondescript pattern. One sinonasal tumor closely mimicked

Address page proofs, correspondence, and requests for reprints to: Abbas Agaimy, MD, Pathologisches Institut, Universitätsklinikum Erlangen, Krankenhausstrasse 8-10, 91054 Erlangen, Germany, Phone: +49-9131-85-22288, Fax: +49-9131-85-24745, abbas.agaimy@uk-erlangen.de.

Conflict of interest: none

nasal chondromesenchymal hamartoma (NCMH). Mitotic activity was low (0 to 5 mitoses/10 hpfs). Immunohistochemical findings were heterogeneous with variable expression of S100 (2/5), EMA (2/3), CD34 (1/4), desmin (1/4) and GFAP (1/3). Targeted RNA sequencing revealed the same *RREB1::MRTFB* fusion in all cases, with exon 8 of *RREB1* being fused to exon 11 of *MRTFB*. This study expands the topographic spectrum of *RREB1::MRTFB* fusion-positive mesenchymal neoplasms, highlighting a significant morphological and phenotypic diversity. Overall, *RREB1::MRTFB*-rearranged neoplasms seem to fall into two subcategories: Tumors with lobulated, chondroid or myxochondroid epithelioid morphology (Case 2 and 3) and those with more undifferentiated hypercellular spindle cell phenotype (Case 1, 4, 5). Involvement of extracranial/extrathoracic sites and the NCMH-like pattern are novel. The biology of these likely indolent or benign tumors remains to be verified in the future.

Keywords

RREB1 ; *MRTFB* ; *MKL2* ; fibromyxoid; perineurioma; sarcoma; soft tissue

INTRODUCTION

Ectomesenchymal chondromyxoid tumor (EMCMT) is a rare, histologically distinctive, site-specific mesenchymal neoplasm of unknown histogenetic origin. Since its first description by Smith et al in 1995 [1], the histogenesis of this tumor has been the subject of ongoing debate. Likewise, its significant predilection (almost exclusive) for the anterior dorsal tongue remains obscure [1]. Smith et al have coined the term “ectomesenchymal chondromyxoid tumor”, based on the assumption that this enigmatic lesion originates from misplaced uncommitted neural crest-derived ectomesenchymal cells [1]. Alternatively, a myoepithelial origin (salivary gland-derived or soft tissue origin) has been proposed by some authors, but rejected by others [2, 3].

To date, no more than 100 cases of EMCMT have been reported in the literature (reviewed in ref. [4, 5, 6]). The neoplastic cells of EMCMT uniformly express vimentin, GFAP and pankeratin with frequent but variable reactivity with S100, smooth muscle actin, p63, and CD57, while desmin, myogenin, synaptophysin and calponin are less commonly expressed, usually with limited reactivity [1, 7, 8].

Recently, Dickson et al reported recurrent *RREB1::MRTFB* (formerly *RREB1::MLK2*) fusions in EMCMT, detected in 90% of cases using targeted RNA sequencing [8]. In contrast, rare cases harbored *EWSR1* rearrangements [8, 9].

While the majority of tumors originate on the anterior dorsum of the tongue, few cases deviated from this and originated from the posterior part or other lateral borders of the tongue instead [1, 8]. Extra-glossal examples of EMCMT are exceedingly rare [10–16] and only five of them have been confirmed by genotyping (Table 1; [13–16]). We herein describe five new tumors carrying this gene fusion including the first two cases originating from extracranial/ extrathoracic soft tissue sites.

MATERIALS AND METHODS

Case 1 was a routine case treated at the University Hospital, Erlangen, Germany. Cases 2 to 5 were identified in the consultation files of the authors (AA, CRA). The tissue specimens were fixed in formalin and processed routinely for histopathology. Due to the consultation nature of the cases, immunohistochemistry (IHC) was performed in different laboratories and the stains applied varied from case to case, based on tissue availability and the initial differential diagnostic considerations (details of the staining protocols and antibody sources are available upon request).

Next generation sequencing

For Cases 1 and 3 – 4, RNA was isolated from formalin-fixed paraffin embedded (FFPE) tissue sections using RNeasy FFPE Kit of Qiagen (Hilden, Germany) and quantified spectrophotometrically using NanoDrop-1000 (Waltham, United States). Molecular analysis was performed using the TruSight RNA Fusion Panel (Illumina, Inc., San Diego, CA, USA) with 500 ng RNA as input according to the manufacturer`s protocol. The library was sequenced on a MiSeq (Illumina, Inc., San Diego, CA, USA) with 3.4 million reads, and sequences were analyzed using the RNA-Seq Alignment workflow, version 2.0.1 (Illumina, Inc., San Diego, CA, USA). The Integrative Genomics Viewer (IGV), version 2.2.13 (Broad Institute, REF) was used for data visualization [17].

Cases 2 and 5 were subjected to targeted RNA sequencing (Archer FusionPlex Custom Solid Panel) to assess for gene fusions. The detailed procedure of Anchored Multiplex PCR RNA sequencing assay has been previously described [18, 19]. Unidirectional gene-specific primers were designed to target specific exons in 123 genes known to be involved in oncogenic fusions in solid tumors.

Fluorescence in-situ hybridization (FISH) on interphase nuclei from paraffin-embedded 4-micron sections was performed applying custom bacterial artificial chromosomes (BAC) probes covering and flanking genes of interest (*RREB1* and *MRTFB*) as previously described [8]. DNA from individual BACs was isolated according to the manufacturer's instructions, labeled with different fluorochromes in a nick translation reaction, denatured, and hybridized to pretreated slides. Slides were then incubated, washed, and mounted with DAPI in an antifade solution, as previously described [20]. The genomic location of each BAC set was verified by hybridizing them to normal metaphase chromosomes. Two hundred successive nuclei were examined using a Zeiss fluorescence microscope (Zeiss Axioplan, Oberkochen, Germany), controlled by Isis 5 software (Metasystems, Newton, MA). A positive score was interpreted when at least 20% of the nuclei showed a split-apart signal in the break-apart assay. Nuclei with incomplete set of signals were omitted from the score.

Based on morphological similarity to Case 3, we tested two additional nasal chondromesenchymal hamartoma (NCMH)-like tumors for fusions using same panel (one case) and the Archer FusionPanel (for the other case). Moreover, all three NCMH-like tumors were tested for the presence of *DICER1* mutations as described previously [21].

RESULTS

Clinical and demographic features

The tumors occurred in three male and two female patients whose age ranged from 18 to 61 years (median, 28) (Table 1). Three tumors were located in the head and neck (one case each in the maxilla, the parapharyngeal space and the posterior nasopharyngeal wall) and two in the soft tissue (one in the right inguinal area and one in the presacral region (representative imaging is shown in Fig. 1A–C)). The tumor size ranged from 3.3 to 20 cm (median, 7). The largest tumor (Case 2) originated in the presacral soft tissue mass abutting but not involving the bone that was resected. Treatment was radical surgical excision in Case 1 and 2, and variable local marginal or nonradical surgical modalities in Case 3 to 5. No adjuvant treatment was given to any of the patients. Case 1 and 4 were disease-free at 17 and 5 months follow-up, respectively; other cases were either recent or have been lost to follow-up.

Pathological findings

All tumors were well circumscribed but non-encapsulated. Their cut-surfaces were described as firm to soft with variable lobulation. Case 1 was diagnosed as unclassified low-grade fibromyxoid neoplasm on initial core needle biopsies (based on non-descript morphology and negative limited immunostains) and primary surgical resection recommended. Other cases were diagnosed initially as low-grade unclassified mesenchymal neoplasms using varying descriptive terms based on immunophenotypes (Cases 2, 4 and 5) and nasal chondromesenchymal hamartoma (Case 3).

Histologically, the soft tissue tumors (Case 1 and 2) shared a predominant fibromyxoid appearance, but with varying cyto-architectural patterns. Case 1 presented as a vaguely lobulated cellular neoplasm composed of slender to focally plump, bland spindle cells arranged in prominent whorls, short fascicles and a storiform pattern with frequent perivascular onionskin pattern (Fig. 2A, B). Focal myxoid stromal change, thickened vessels surrounded by concentric neoplastic cells (Fig. 2C, D), focal rhythmic arrangement of the nuclei alternating with paucicellular trabeculae (Fig. 2E, F), and large foci of ischemic type necrosis were present.

At low power, Case 2 showed variable lobulation with several small lobules embedded within a chondromyxoid background stroma (Fig. 3A–C). The neoplastic cells were predominantly plump ovoid to medium-sized to large epithelioid cells with well demarcated, variably vacuolated (Fig. 3D) or pale granular cytoplasm (Fig. 3E). Numerous intranuclear pseudoinclusions were noted (Fig. 3E). A variable spindle cell component was seen, occasionally with prominent degenerative cytological atypia (Fig. 3F).

Case 3 was strikingly similar to NCMH with multiple smaller lobules of primitive chondromyxoid tissue entrapping mature bone trabeculae and scattered foci of fat with a frequent concentric arrangement of the myxoid nodules (Fig. 4). Case 4 was highly cellular composed of a nondescript arrangement of spindled to ovoid and round cells with variable fascicular to storiform patterns of growth, pericytoma-like vasculature and prominent cystic features (Fig. 5). Case 5 showed diffusely confluent nests and sheets of monomorphic ovoid

and focally spindled to fusiform cells with variable pseudofollicular spaces containing pale stained oedematous vacuolated secretory material (Fig. 6). Focal gaping vessels were noted in the spindle cell areas. All cases lacked coagulative necrosis and significant atypia. Mitotic activity was low, ranging from 0 to 5 mitoses/10 hpfs.

Immunohistochemical finings

Immunohistochemical findings were overall heterogeneous with variable expression of S100 (2/5), EMA (2/3), CD34 (1/4), synaptophysin (1/1), desmin (1/4), MyoD1 (1/2), myogenin (1/2) and GFAP (1/3).

Case 1 revealed prominent but variable expression of CD34 (diffuse in some lobules and negative or variable in others, Fig. 7A, B). EMA was expressed in <5% of the neoplastic cells (Fig. 7C). Very few cells expressed Claudin1. Case 2 showed diffuse strong expression of S100 (Fig. 7D) as well as CD68 and EMA (Fig. 7E) in rare cells. Moreover, Case 4 revealed strong and diffuse expression of synaptophysin (Fig. 7F). Case 3 strongly expressed S100 and weakly SATB2. Remarkably, the nasopharyngeal wall tumor (Case 5) revealed prominent expression of MyoD1 (Fig. 6D, main image) and focal reactivity for desmin (Fig. 6D, subimage) and myogenin, indicating partial rhabdomyoblastic differentiation. Other markers as listed in Table 2 (including SOX10) tested negative.

Molecular results

All five tumors revealed a *RREB1::MRTFB* gene fusion (Table 2). In all cases, the fusion gene contained exons 1 to 8 of *RREB1* and exons 11 to 17 of *MRTFB* (Fig. 8). FISH analysis confirmed the rearrangements of both genes (Fig. 9).

Nasal chondromesenchymal hamartoma-like tumors

As one sinonasal tumor (Case 3) was strikingly similar to and initially diagnosed as nasal chondromesenchymal hamartoma (NCMH), we have tested two additional cases with similar histology to verify if these might belong to the same tumor spectrum. Case 3 occurred in a 28-year-old female in the jaw. The two additional NCMH-like tumors affected one female and one male aged 4 and 14 years, respectively. They originated in the nose and ethmoid/ maxillary sinus. Histologically, all three tumors displayed a stereotypical NCMH-like histology with a predominance of variably mature or primitive myxoid cartilage forming variably sized microlobules and blending with slightly cellular diffuse chondromyxoid stroma. Variable degree of concentric arrangement was seen in two cases and a fatty component in one. The lesion from the child showed more prominent and mature appearing bone formation. There was no epithelial component, entrapped glands, mitoses or atypia. Immunohistochemistry revealed consistent expression of S100 but no other lineage-specific or epithelial markers were expressed. All tumors were classified as NCMH, but they lacked pathogenic *DICER1* mutations or other mutations in the 160 genes included in the panel used. Of these three *DICER1*-wild type cases, one revealed a *RREB1::MRTFB* fusion (Case 3 in table 1) and the other two had no detectable fusions. The clinicopathologic features of NCMH-like tumors are summarized in Table 3. Representative images of the fusion-positive case are depicted in Figure 4.

DISCUSSION

The *RREB1::MRTFB* (former *RREB1::MKL2)* fusion has emerged recently as a defining feature in most if not all of ectomesenchymal chondromyxoid tumors (EMCMT) of the tongue. Dickson et al detected this fusion in 19 of 21 tumors (90%) [8]. A single tumor (5%) had an *EWSR1::CREM* fusion, and the remaining case lacked any known fusion gene by RNA Sequencing [8]. In addition, *EWSR1* rearrangements (fusion partner unknown) have been detected by FISH in 27% of 11 cases in one study [9]. Notably the *EWSR1::CREM* fusion-positive case lacked all of the characteristic immunomarkers of EMCMT [8]. Whether these *EWSR1*-rearranged cases represent genetic variants of EMCMT or are more related to the *EWSR1::CREM* fusion family neoplasms remains currently controversial [8,9,22].

The *MRTFB* gene (AKA: *MKL2* or *Myocardin Like 2*), mapped to 16p13.12, encodes for the *Myocardin Related Transcription Factor B* [23]. MRTFB is a transcription coactivator of serum response factor, involved in developmental processes such as smooth and skeletal muscle differentiation and in neuronal development [23–25]. In general, *MRTFB* (*MKL2*) fusions are uncommon. In the soft tissue, *MRTFB* (*MKL2*) is fused to C11orf95 in the majority of chondroid lipomas [26], a rare soft tissue neoplasm with subtle morphological similarities to EMCMT; both being characterized by prominent myxoid or chondromyxoid matrix.

The *RREB1* gene, mapped to 6p24.3, encodes for the *Ras-Responsive Element-Binding Protein 1* [27]. This Kruppel-like protein from the zinc finger protein family has been originally isolated in a human medullary thyroid carcinoma cell line [27]. Via stimulation of the transcription of down-stream target genes, RREB1 influences vital processes such as cell proliferation, differentiation, tumorigenesis and metastasis [27]. Notably, genes associated with extracellular matrix proteases might be regulated via the Ras proteins, which are in turn under the influence of RREB1 [27]. Except for EMCMTs, *RREB1* fusions are exceptionally rare in solid tumors. Complex *RREB1::CMAHP* and *ELL::RREB1* fusions, concurrent with other translocations, have been described in a case of infantile acute myeloid leukemia [28].

EMCMTs usually are composed of uniform ovoid or fusiform cells forming multiple closely packed lobules with frequent multilobated nuclei and scattered atypical cells, embedded in a chondromyxoid background [1,7,8,15]. The cells of EMCMT stain diffusely with GFAP and pankeratin, but less frequently with S100 and SMA. Desmin expression is uncommon. Although the above features characterize the prototypical tumors, uncommon or unusual features have been encountered in a few cases, either focally or diffusely. These include hypercellularity, hyalinized stroma and necrosis [8].

To date, very few cases of extra-glossal EMCMT have been reported [10–16]. However, only five genuine extra-glossal EMCMTs have been verified by molecular testing (Table 1 and 2). These tumors originated predominantly in females (4:1) at a mean age of 53 years (range, 25 – 73) and involved exclusively head and neck (3 cases; parapharyngeal, sinonasal and mandibular [13,15,16]) and mediastinal (2 cases [14]) sites. Including our cases, a total of 10 molecularly verified extraglossal *RREB1::MRTFB*-rearranged neoplasms

have been documented. Their ages ranged from 18 to 73 years (median, 36); 60% were females. Six of 10 cases were located in head and neck sites (two parapharyngeal, two in the jaw, one nasopharyngeal and one sinonasal). The remainder were either mediastinal (2) or have originated in extra-glossal, extra-mediastinal soft tissue sites (2); the latter two cases represent a novel location for these tumors. Following surgical treatment alone, all five patients with follow-up (range, 5 – 27 months; median, 17) were disease free indicating an indolent behavior. The immunophenotypes of these tumors varied greatly with variable expression of S100 (7/10), SMA (5/7), EMA (5/7), GFAP (4/7), desmin (3/9), myogenin (2/6), and AE1/AE3 (2/8) (Table 2). The two tumors with variable rhabdomyoblastic differentiation originated in the retro-/parapharyngeal space and the posterior nasopharyngeal wall. Notably, two tumors with *RREB1::MRTFB* fusion and myogenic differentiation were previously reported as biphenotypic sinonasal sarcoma [13].

These extra-glossal tumors showed variable resemblance to glossal EMCMTs but were dominated by variant histology including hypercellular nodules arranged into sheets and fascicles and hypocellular areas arranged into cords, reticular pattern, or haphazardly within a hyalinized stroma. Cellular storiform proliferation of bland spindle cells with perivascular hyalinization and occasional nuclear pseudoinclusions as well as myxoid areas containing round to polygonal cells and scattered binucleated cells were observed as well [13–16]. Overall, *RREB1::MRTFB*-rearranged neoplasms seem to fall into two morphological subcategories: Tumors with lobulated, chondroid or myxochondroid epithelioid phenotype (seen in 3 cases) and tumors with more undifferentiated hypercellular spindle cell morphology (seen in 7 cases; Table 2).

Currently, it remains controversial, whether these extra-glossal *RREB1::MRTFB*-rearranged neoplasms do represent genuine extra-glossal counterparts of EMCMT or they merely represent genetic variants in the spectrum of different site-specific independent entities. This controversy is reflected by the names used for them by different authors (e.g. BSS) and is mainly due to the variant histology and immunophenotype among reported cases.

Notably, several uncommon variant features reported in genuine EMCMT of the tongue were observed in most of our current cases. These uncommon features include the presence of cellular spindle cell areas showing a vaguely fascicular growth pattern and tumors with prominent eosinophilic hyaline stroma with superficial resemblance to hyaline cartilage. The first feature represents the predominant pattern seen in our Case 1 and 4, while the second was predominant in Case 2. This confirms at least some degree of analogy of the current cases with variant glossal EMCMT. However, the prominent granular cell pattern seen in Case 2 is unusual and potentially misleading. Moreover, the striking resemblance of one of our cases to perineurioma histologically and immunohistochemically (prominent expression of CD34 and limited focal reactivity for EMA and claudin1) is noteworthy. A perineurioma-like morphology with or without expression of perineurial markers has been reported in other translocation-associated sarcomas such as low-grade fibromyxoid sarcoma, representing a diagnostic pitfall [29]. Moreover, a recent study by Dickson et al identified a high frequency of *VGLL3* gene fusions in tumors in the spectrum of hybrid schwannoma-perineurioma (detected in 14 of 18 cases) [30]. *CHD7* (n=10), *CHD9* (n=2), and *MAMLD1* (n=2) were the partner genes encountered [30]. In addition, novel *DST::BRAF* and

SQSTM1::CDX1 fusions were detected in two cases, while two tumors lacked identifiable fusions [30]. The authors suggested that hybrid schwannoma–perineurioma likely represents a distinct entity, unrelated to conventional schwannoma and perineurioma [30]. One of our cases illustrates the limited specificity of the perineurioma-like immunophenotype.

Two other findings in our series merit special attention. Case 3 was very similar to NCMH and indeed this was the original diagnosis. NCMH is a rare sinonasal lesion with strong association with the DICER1 syndrome [31,32]. The vast majority of affected patients are newborns or young children [31–34]. However, the cases we examined herein were diagnosed at an older age compared to the vast majority of NCMH. Moreover, the one harboring the *RREB1::MRTFB* fusion affected an adult. Although the morphology of these tumors is very similar to reported NCMH, it is possible that these tumors represent a distinctive chondromyxoid tumor unrelated to the DICER1 syndrome as evidenced by lack of *DICER1* mutations in all three cases and instead presence of *RREB1::MRTFB* fusion in one of them. Analysis of more cases should shed light on the nosology and histogenesis of this distinctive lesion.

The two cases we reported from non-head-and-neck soft tissue sites are novel. Their morphology overlaps variably with glossal EMCMT and with variant extraglossal cases. Nevertheless, the morphological diversity of these tumors rather argues for potentially different entities unified by the presence of the *RREB1::MRTFB* fusion than for different faces of the same entity, but this remains a controversial issue to be addressed in future studies if more cases are reported. Their differential diagnosis includes a wide range of low-grade neoplasms showing fibromyxoid or chondromyxoid patterns as well as perineurial cell lesions. In particular, myoepithelial neoplasms, nerve sheath myxoma, extraskeletal myxoid chondrosarcoma and ossifying fibromyxoid tumor of soft parts need be ruled out by defined demographic, morphological, immunophenotypic, and genetic criteria.

Of interest, our Case 5 showed histological features potentially overlapping with BSS with rhabdomyoblastic differentiation [35–38]. Moreover, two tumors with identical *RREB1::MRTFB* fusion were reported previously as BSS [13,16]. However, there is no proof that these tumors represent genuine BSS as their immunophenotype is highly heterogeneous and may overlap with more than one entity including BSS. Notably, BSS, including also those cases with rhabdomyoblastic differentiation, is driven by *PAX3* fusions (mostly fused to *MAML3*, less frequently to *FOXO1*, and rarely to *NCOA2/1* and *WWTR1*) and they have not been reported to harbor the *RREB1::MRTFB* fusion [35–38].

In summary, we have described five *RREB1::MRTFB*-positive extraglossal mesenchymal neoplasms bringing up the total number of reported cases to 10. Our study for the first time documents the occurrence of these tumors in extraglossal, extra-mediastinal soft tissue sites. From the reported cases, it seems that these extraglossal *RREB1::MRTFB* fusion-driven neoplasms are biologically indolent with predilection for the head and neck soft tissue in adults with slight overrepresentation of females. These neoplasms do not fit exactly any defined tumor entity, but show some overlap with reported extra-glossal EMCMT. A potential relationship of the NCMH-like cases to genuine NCMH remains to be

verified. Moreover, identification of more cases is mandatory to delineate the morphological spectrum and the biological behavior of this rare entity.

Funding:

Supported in part by: P50 CA217694 (CRA), P50 CA140146 (CRA), P30 CA008748 (CRA), Cycle for Survival (CRA).

REFERENCES

1. Smith BC, Ellis GL, Meis-Kindblom JM, Williams SB. Ectomesenchymal chondromyxoid tumor of the anterior tongue. Nineteen cases of a new clinicopathologic entity. Am J Surg Pathol. 1995;19:519–30. [PubMed: 7726361]
2. Nikitakis NG, Argyris P, Sklavounou A, Papadimitriou JC. Oral myoepithelioma of soft tissue origin: report of a new case and literature review. Oral Surg Oral Med Oral Pathol Oral Radiol Endod. 2010;110:e48–51. [PubMed: 20955943]
3. Goveas N, Ethunandan M, Cowlishaw D, Flood TR. Ectomesenchymal chondromyxoid tumour of the tongue: Unlikely to originate from myoepithelial cells. Oral Oncol. 2006;42:1026–8. [PubMed: 17011812]
4. Aldojain A, Jaradat J, Summersgill K, Bilodeau EA. Ectomesenchymal Chondromyxoid Tumor: A Series of Seven Cases and Review of the Literature. Head Neck Pathol. 2015;9:315–22. [PubMed: 25404177]
5. Truschnegg A, Acham S, Kqiku L, Jakse N, Beham A. Ectomesenchymal chondromyxoid tumor: a comprehensive updated review of the literature and case report. Int J Oral Sci. 2018;10(1):4. [PubMed: 29491357]
6. Naidoo S, Roode GJ, Bütow KW, Meer S. Ectomesenchymal Chondromyxoid Tumor: A Rare Association With an Asymmetrical Soft Palate Cleft. Cleft Palate Craniofac J. 2021 Aug 30:10556656211035029.
7. Laco J, Mottl R, Höbling W, Ihrler S, Grossmann P, Skalova A, Ryska A. Cyclin D1 Expression in Ectomesenchymal Chondromyxoid Tumor of the Anterior Tongue. Int J Surg Pathol. 2016;24:586–94. [PubMed: 27240862]
8. Dickson BC, Antonescu CR, Argyris PP, Bilodeau EA, Bullock MJ, Freedman PD, Gnepp DR, Jordan RC, Koutlas IG, Lee CH, Leong I, Merzianu M, Purgina BM, Thompson LDR, Wehrli B, Wright JM, Swanson D, Zhang L, Bishop JA. Ectomesenchymal Chondromyxoid Tumor: A Neoplasm Characterized by Recurrent RREB1-MKL2 Fusions. Am J Surg Pathol. 2018;42:1297–1305. [PubMed: 29912715]
9. Argyris PP, Bilodeau EA, Yancoskie AE, Trochesset D, Pambuccian SE, Wetzel SL, Shah SS, Edelman M, Freedman P, Dolan M, Koutlas IG. A subset of ectomesenchymal chondromyxoid tumours of the tongue show EWSR1 rearrangements and are genetically linked to soft tissue myoepithelial neoplasms: a study of 11 cases. Histopathology. 2016;69:607–13. [PubMed: 27010880]
10. Nigam S, Dhingra KK, Gulati A. Ectomesenchymal chondromyxoid tumor of the hard palate--a case report. J Oral Pathol Med. 2006;35:126–8. [PubMed: 16430745]
11. Gouvêa AF, Díaz KP, Léon JE, Vargas PA, de Almeida OP, Lopes MA. Nodular lesion in the anterior hard palate. Oral Surg Oral Med Oral Pathol Oral Radiol. 2012;114:154–9. [PubMed: 22769404]
12. Stecco A, Quagliozzi M, Pino M, Spina P, Pia F, Boldorini R, Carriero A. An unusual case of ectomesenchymal chondromyxoid tumour of the left tonsillar bed: imaging and histopathologic features. BJR Case Rep. 2016;2:20150183. [PubMed: 30459964]
13. Siegfried A, Romary C, Escudié F, Nicaise Y, Grand D, Rochaix P, Barres B, Vergez S, Chevreau C, Coindre JM, Uro-Coste E, Le Guellec S. RREB1-MKL2 fusion in biphenotypic "oropharyngeal" sarcoma: New entity or part of the spectrum of biphenotypic sinonasal sarcomas? Genes Chromosomes Cancer. 2018;57:203–210. [PubMed: 29266774]

14. Makise N, Mori T, Kobayashi H, Nakagawa K, Ryo E, Nakajima J, Kohsaka S, Mano H, Aburatani H, Yoshida A, Ushiku T. Mesenchymal tumours with RREB1-MRTFB fusion involving the mediastinum: extra-glossal ectomesenchymal chondromyxoid tumours? Histopathology. 2020;76:1023–1031. [PubMed: 31991003]
15. Bubola J, Hagen K, Blanas N, Weinreb I, Dickson BC, Truong T. Expanding Awareness of the Distribution and Biologic Potential of Ectomesenchymal Chondromyxoid Tumor. Head Neck Pathol. 2021;15:319–322. [PubMed: 32372271]
16. Mechtersheimer G, Andrulis M, Delank KW, Volckmar AL, Zhang L, von Winterfeld M, Stenzinger A, R Antonescu C. RREB1-MKL2 fusion in a spindle cell sinonasal sarcoma: biphenotypic sinonasal sarcoma or ectomesenchymal chondromyxoid tumor in an unusual site? Genes Chromosomes Cancer. 2021;60:565–570. [PubMed: 33715240]
17. Robinson JT, Thorvaldsdóttir H, Winckler W, Guttman M, Lander ES, Getz G, Mesirov JP. Integrative Genomics Viewer. Nature Biotechnology 2011;29:24–26.
18. Zheng Z, Liebers M, Zhelyazkova B, Cao Y, Panditi D, Lynch KD, Chen J, Robinson HE, Shim HS, Chmielecki J, Pao W, Engelman JA, Iafrate AJ, Le LP. Anchored multiplex PCR for targeted next-generation sequencing. Nat Med. 2014;20:1479–84. [PubMed: 25384085]
19. Zhu G, Benayed R, Ho C, Mullaney K, Sukhadia P, Rios K, Berry R, Rubin BP, Nafa K, Wang L, Klimstra DS, Ladanyi M, Hameed MR. Diagnosis of known sarcoma fusions and novel fusion partners by targeted RNA sequencing with identification of a recurrent ACTB-FOSB fusion in pseudomyogenic hemangioendothelioma. Mod Pathol. 2019;32:609–620. [PubMed: 30459475]
20. Antonescu CR, Zhang L, Chang NE, Pawel BR, Travis W, Katabi N, Edelman M, Rosenberg AE, Nielsen GP, Dal Cin P, Fletcher CD. EWSR1-POU5F1 fusion in soft tissue myoepithelial tumors. A molecular analysis of sixty-six cases, including soft tissue, bone, and visceral lesions, showing common involvement of the EWSR1 gene. Genes Chromosomes Cancer. 2010;49:1114–24. [PubMed: 20815032]
21. Agaimy A, Witkowski L, Stoehr R, Cuenca JCC, González-Muller CA, Brütting A, Bährle M, Mantsopoulos K, Amin RMS, Hartmann A, Metzler M, Amr SS, Foulkes WD, Sobrinho-Simões M, Eloy C. Malignant teratoid tumor of the thyroid gland: an aggressive primitive multiphenotypic malignancy showing organotypical elements and frequent DICER1 alterations-is the term “thyroblastoma” more appropriate? Virchows Arch. 2020;477:787–798. [PubMed: 32507920]
22. Yoshida A, Wakai S, Ryo E, Miyata K, Miyazawa M, Yoshida KI, Motoi T, Ogawa C, Iwata S, Kobayashi E, Watanabe SI, Kawai A, Mori T. Expanding the Phenotypic Spectrum of Mesenchymal Tumors Harboring the EWSR1-CREM Fusion. Am J Surg Pathol. 2019;43:1622–1630. [PubMed: 31305268]
23. Selvaraj A, Prywes R. Megakaryoblastic leukemia-1/2, a transcriptional co-activator of serum response factor, is required for skeletal myogenic differentiation. J Biol Chem. 2003;278:41977–87. [PubMed: 14565952]
24. Cen B, Selvaraj A, Prywes R. Myocardin/MKL family of SRF coactivators: key regulators of immediate early and muscle specific gene expression. J Cell Biochem. 2004;93:74–82. [PubMed: 15352164]
25. Mokalled MH, Johnson A, Kim Y, Oh J, Olson EN. Myocardin-related transcription factors regulate the Cdk5/Pctaire1 kinase cascade to control neurite outgrowth, neuronal migration and brain development. Development. 2010;137:2365–74. [PubMed: 20534669]
26. Huang D, Sumegi J, Dal Cin P, Reith JD, Yasuda T, Nelson M, Muirhead D, Bridge JA. C11orf95-MKL2 is the resulting fusion oncogene of t(11;16)(q13;p13) in chondroid lipoma. Genes Chromosomes Cancer. 2010;49:810–8. [PubMed: 20607705]
27. Thiagalingam A, De Bustros A, Borges M, Jasti R, Compton D, Diamond L, Mabry M, Ball DW, Baylin SB, Nelkin BD. RREB-1, a novel zinc finger protein, is involved in the differentiation response to Ras in human medullary thyroid carcinomas. Mol Cell Biol. 1996;16:5335–45. [PubMed: 8816445]
28. Tuborgh A, Meyer C, Marschalek R, Preiss B, Hasle H, Kjeldsen E. Complex three-way translocation involving MLL, ELL, RREB1, and CMAHP genes in an infant with acute myeloid leukemia and t(6;19;11)(p22.2;p13.1;q23.3). Cytogenet Genome Res. 2013;141:7–15. [PubMed: 23735562]

29. Thway K, Fisher C, Debiec-Rychter M, Calonje E. Claudin-1 is expressed in perineurioma-like low-grade fibromyxoid sarcoma. Hum Pathol. 2009;40:1586–90. [PubMed: 19540561]
30. Dickson BC, Antonescu CR, Demicco EG, Leong DI, Anderson ND, Swanson D, Zhang L, Fletcher CDM, Hornick JL. Hybrid schwannoma-perineurioma frequently harbors VGLL3 rearrangement. Mod Pathol. 2021;34:1116–1124. [PubMed: 33649458]
31. González IA, Stewart DR, Schultz KAP, Field AP, Hill DA, Dehner LP. DICER1 tumor predisposition syndrome: an evolving story initiated with the pleuropulmonary blastoma. Mod Pathol 2022;35:4–22. [PubMed: 34599283]
32. Stewart DR, Messinger Y, Williams GM, Yang J, Field A, Schultz KA, Harney LA, Doros LA, Dehner LP, Hill DA. Nasal chondromesenchymal hamartomas arise secondary to germline and somatic mutations of DICER1 in the pleuropulmonary blastoma tumor predisposition disorder. Hum Genet 2014;133:1443–50. [PubMed: 25118636]
33. Vasta LM, Nichols A, Harney LA, Best AF, Carr AG, Harris AK, Miettinen M, Schultz KAP, Kim HJ, Stewart DR. Nasal chondromesenchymal hamartomas in a cohort with pathogenic germline variation in DICER1. Rhinol Online. 2020;3:15–24. [PubMed: 34164613]
34. McDermott MB, Ponder TB, Dehner LP. Nasal chondromesenchymal hamartoma: an upper respiratory tract analogue of the chest wall mesenchymal hamartoma. Am J Surg Pathol 1998;22:425–33. [PubMed: 9537469]
35. Wang X, Bledsoe KL, Graham RP, Asmann YW, Viswanatha DS, Lewis JE, Lewis JT, Chou MM, Yaszemski MJ, Jen J, Westendorf JJ, Oliveira AM. Recurrent PAX3-MAML3 fusion in biphenotypic sinonasal sarcoma. Nat Genet. 2014;46:666–8. [PubMed: 24859338]
36. Wong WJ, Lauria A, Hornick JL, Xiao S, Fletcher JA, Marino-Enriquez A. Alternate PAX3-FOXO1 oncogenic fusion in biphenotypic sinonasal sarcoma. Genes Chromosomes Cancer. 2016;55:25–9. [PubMed: 26355893]
37. Huang SC, Ghossein RA, Bishop JA, Zhang L, Chen TC, Huang HY, Antonescu CR. Novel PAX3-NCOA1 Fusions in Biphenotypic Sinonasal Sarcoma With Focal Rhabdomyoblastic Differentiation. Am J Surg Pathol. 2016;40:51–9. [PubMed: 26371783]
38. Fritchie KJ, Jin L, Wang X, Graham RP, Torbenson MS, Lewis JE, Rivera M, Garcia JJ, Schembri-Wismayer DJ, Westendorf JJ, Chou MM, Dong J, Oliveira AM. Fusion gene profile of biphenotypic sinonasal sarcoma: an analysis of 44 cases. Histopathology. 2016;69:930–936. [PubMed: 27454570]

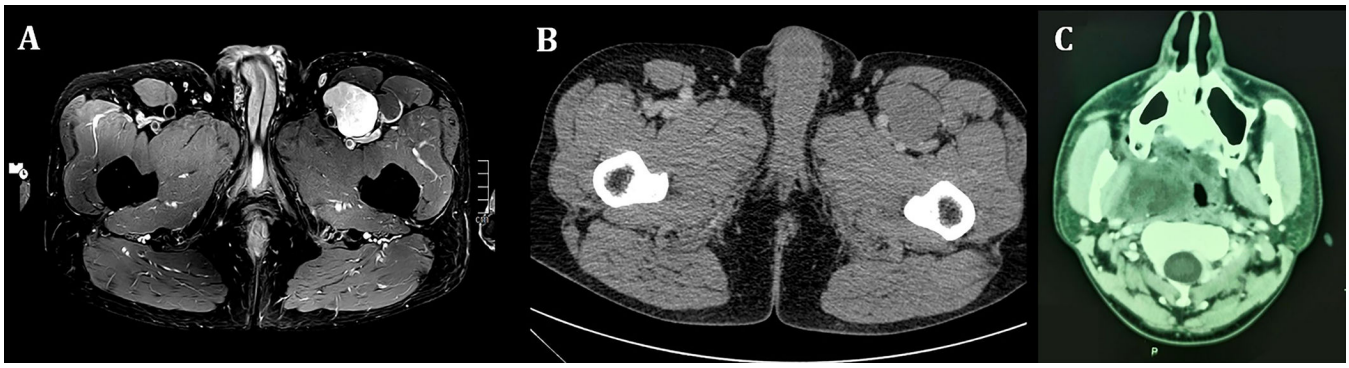

FIGURE 1.

Representative radiological images of extra-glossal *RREB1::MRTFB*-positive neoplasms. **A** (magnetic resonance imaging of Case 1): A PDW TSE SPAIR axial image shows a well circumscribed, heterogeneously hyperintense mass in the left anterior thigh with contact to the femoral artery and vein (PDW=proton density-weighted; TSE=Turbo Spin Echo; SPAIR=SPectral Attenuated Inversion Recovery). **B**: Computed tomography (CT) of the pelvis (same Case) shows an isodense soft tissue mass with sharp margins and contact to the femoral artery and vein as well as to the sartorius and the rectus femoris. **C**: Axial post-contrast CT through the level of the maxillary sinus in Case 4. An ill-defined, inhomogeneous, partly cystic soft tissue mass in the right masticator space with lateral displacement of the medial pterygoid muscle, medial displacement of the pharynx, and contact to the carotid space.

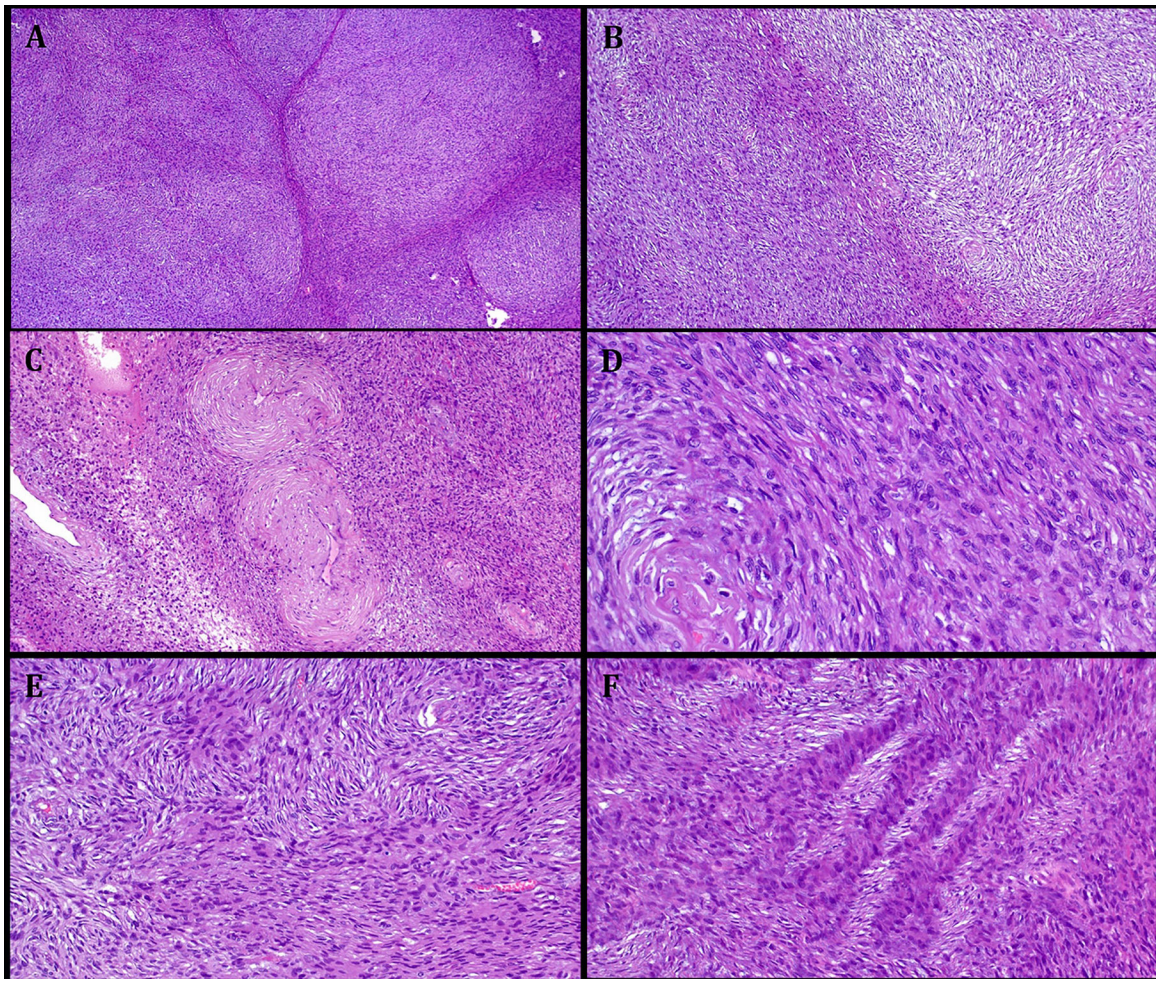

FIGURE 2.

Representative images illustrating the histological features in Case 1. **A**: at low power, a cellular lobulated neoplasm is seen. **B**: abrupt transition from myxoid to non-myxoid cellular areas. **C**: thickened vessels surrounded by concentric neoplastic cells. **D**: high power shows elongated slender spindle cells, note perineurioma-like perivascular whorls. **E**: prominent storiform pattern with pale stained and moderately eosinophilic alternating fascicles cut transversally. **F**: distinct alternation of pale stained and moderately eosinophilic fascicles cut longitudinally.

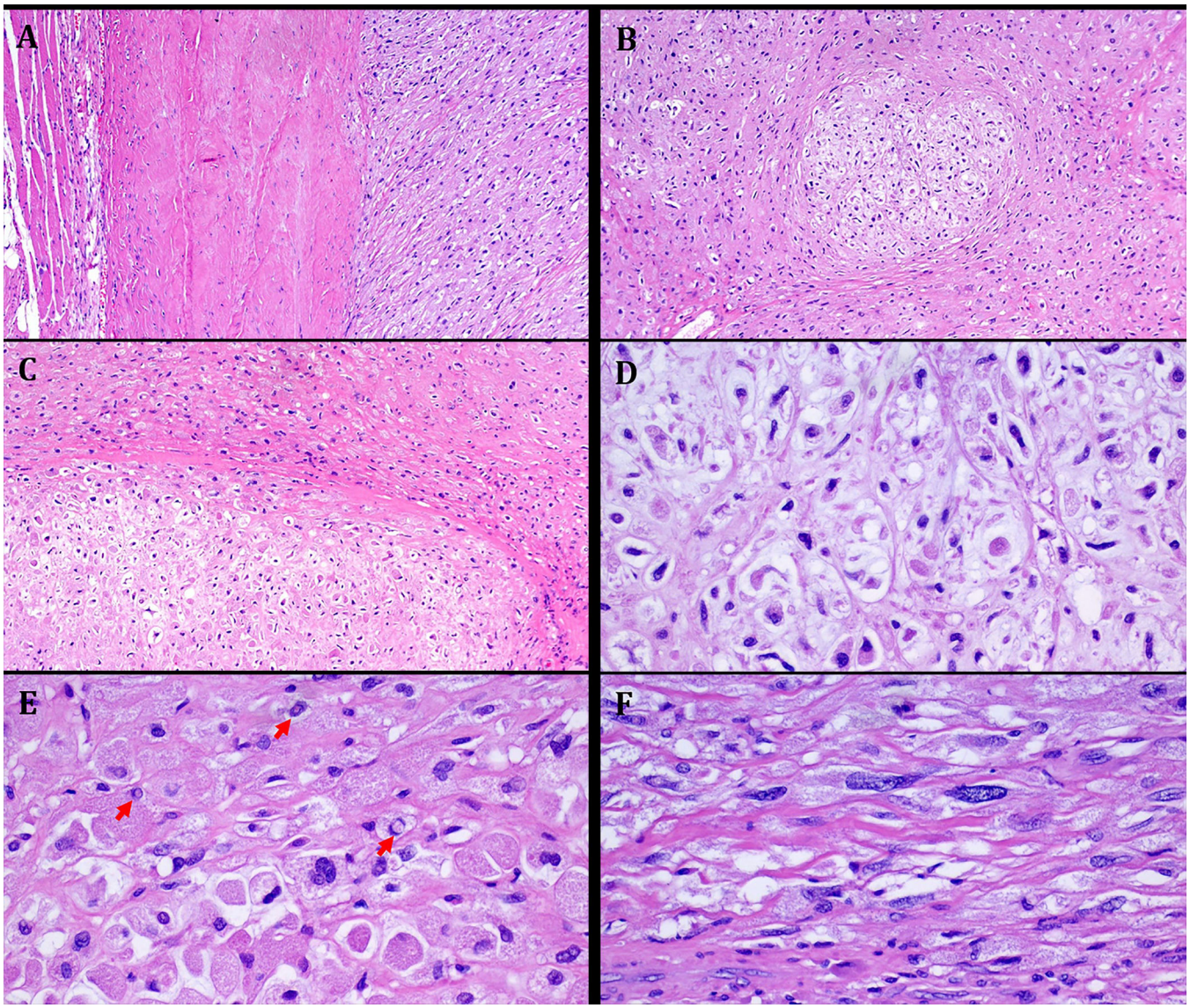

FIGURE 3.

Representative images illustrating the histological features in Case 2. **A**. well-circumscribed tumor periphery surrounded by fascia and muscle on left. **B**: at low power, chondromyxoid lobules are seen embedded within hyaline variably sclerosed stroma. **C**: higher magnification showing abrupt transition between chondromyxoid and hyaline areas. **D**: admixture of large epithelioid variably vacuolated tumor cells and scattered spindle cells seen at high power. **E**: prominent eosinophilic and granular cytoplasmic quality, note numerous nuclear pseudoinclusions (arrows). **F**: scattered spindle cells with hyperchromatic atypical looking nuclei.

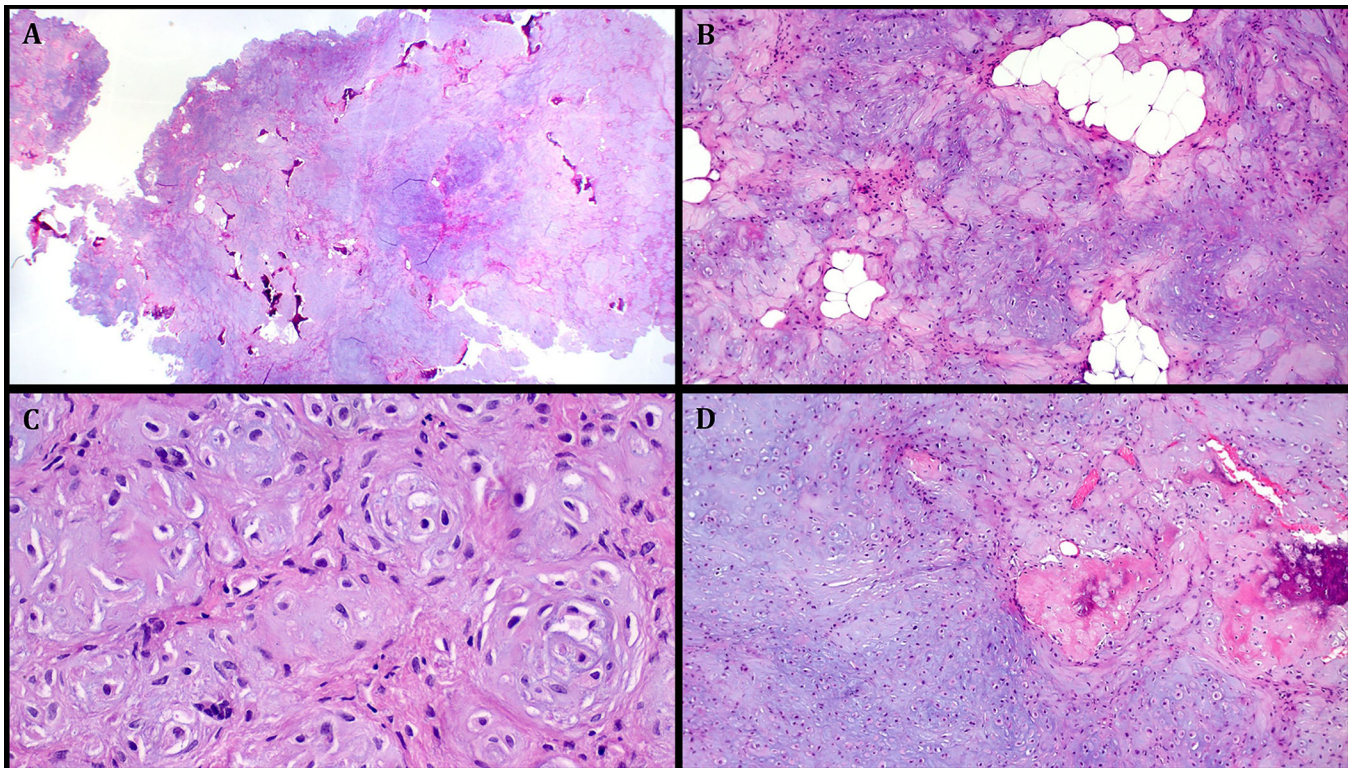

FIGURE 4.

Representative images illustrating the histological features in Case 3. **A**: large partially polypoid chondromyxoid mass with scattered bone islands seen at low power. **B**: prominent microlobulation with islands of mature fat. **C**: higher magnification showing concentric arrangements of mcirolobules with intervening primitive fibroblastic-like spindled mesenchymal cells. **D**: Focus of bone merging with immature chondromyxoid mesenchymal tissue.

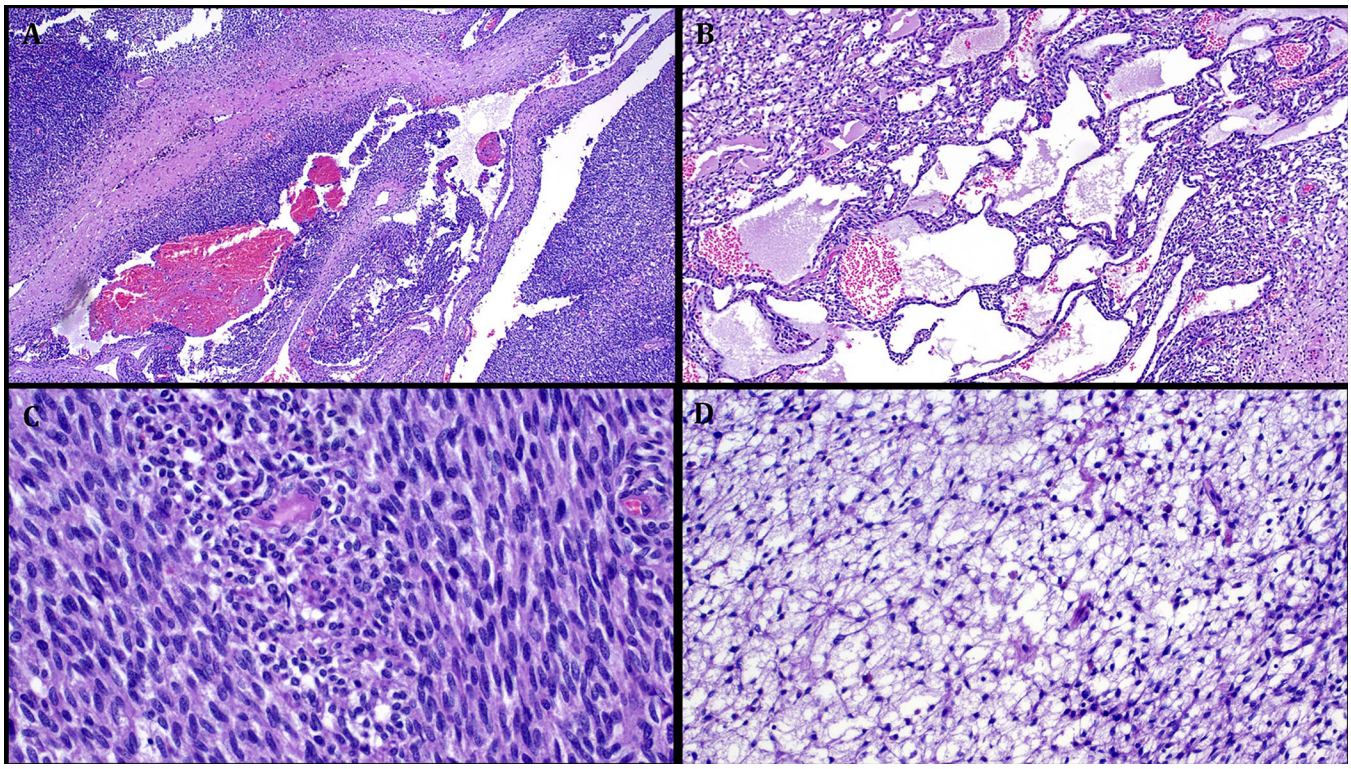

FIGURE 5.

Representative images illustrating the histological features in Case 4. **A**: low power view showing highly cellular neoplasm with alternating solid and cystic areas. **B**: prominent macrocystic stromal degeneration. **C**: highly cellular fibrosarcoma-like areas (with little to no mitoses). **D**: prominent primitive reticular-myxoid stromal features reminiscent of EMCMT of tongue.

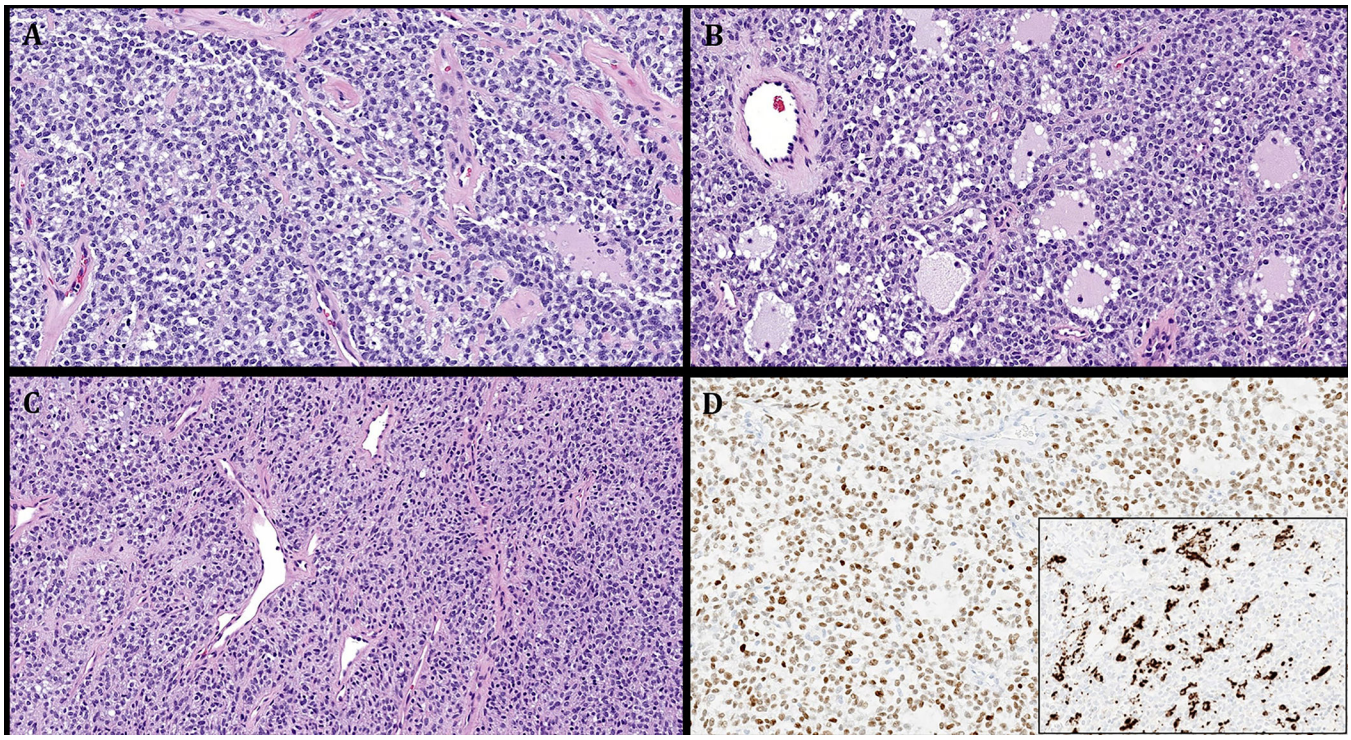

FIGURE 6.

Representative images illustrating the histological features in Case 5. **A**: monotonous round to ovoid bland cells arranged into non-descript confluent sheets. **B**: prominent pseudofollicular spaces are seen. **C**: cellular spindle cell areas with thin-walled gaping vessels. **D**: main image: diffuse expression of MyoD1. Subimage: variable expression of desmin.

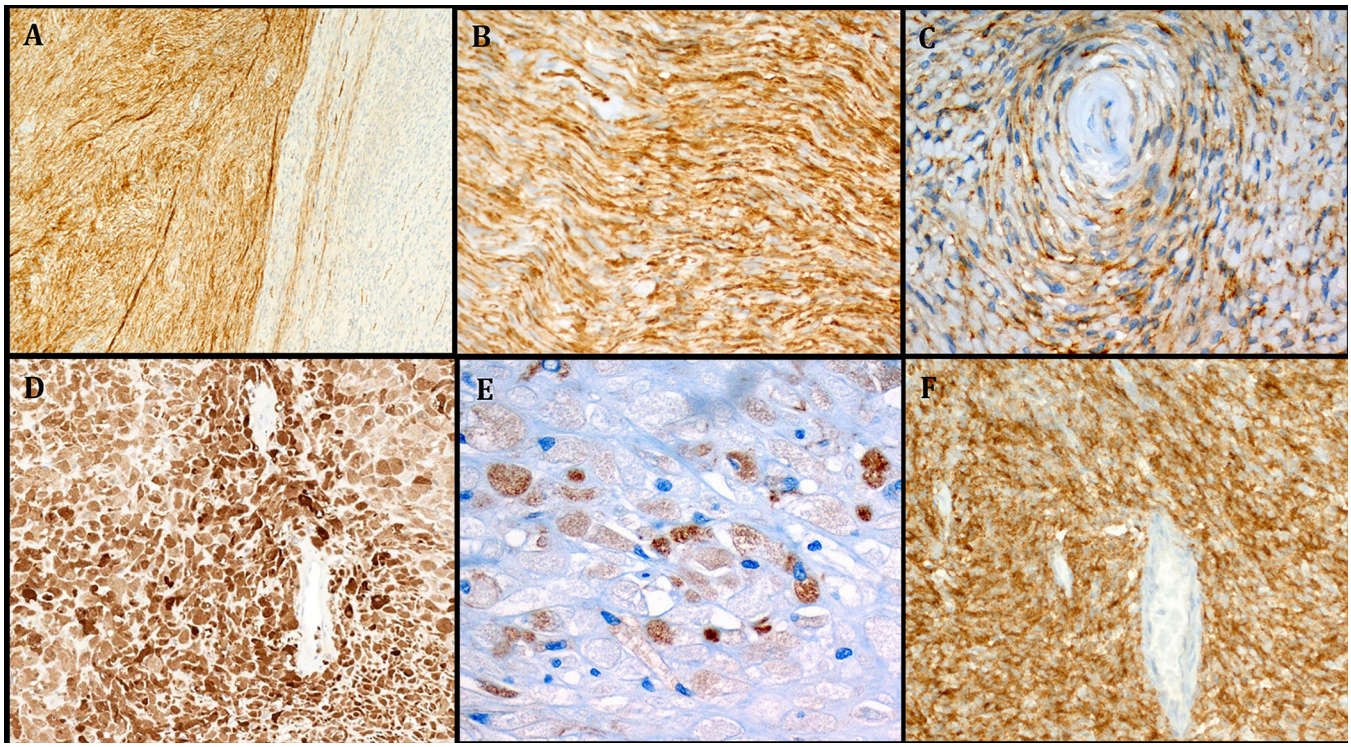

FIGURE 7.

A: Immunohistochemistry showed strong expression of CD34 in some but not all lobules in Case 1. **B**: higher magnification of **A** highlighting the perineurioma-like CD34 pattern. **C**: focal EMA expression in the perivascular whorls (same case). **D**: Case 2 showed strong and diffuse S100 expression. **E**: scattered tumor cells stained for EMA (Case 2). **F**: Case 4 showed diffuse and strong expression of synaptophysin.

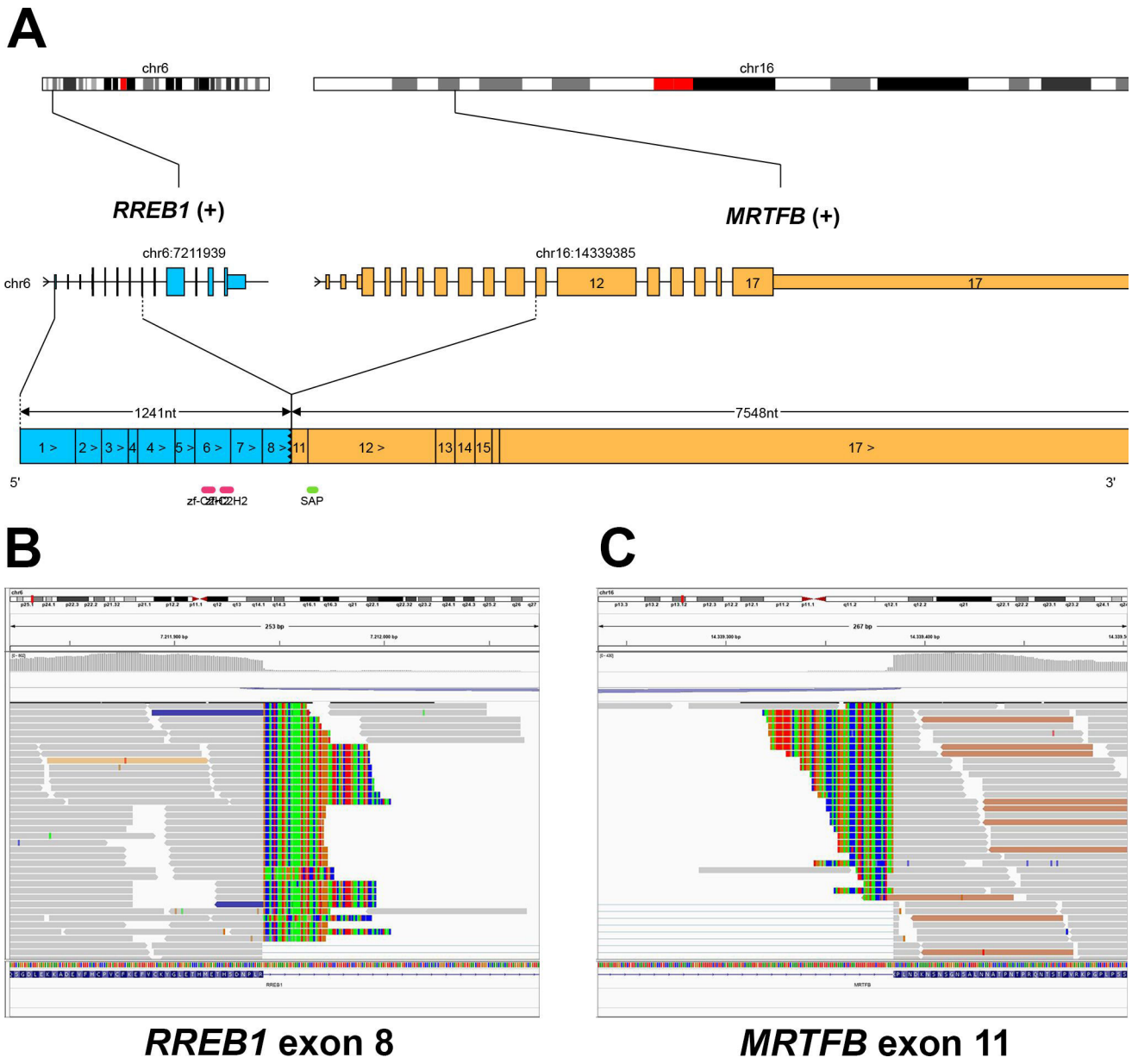

FIGURE 8.

Graphical representation of the *RREB1*::*MRTFB* gene fusion (Case 1). The fusion gene comprised exons 1 to 8 of *RREB1* and exons 11 to 17 of *MRTFB* (**A**). Representative IGV screenshots demonstrating split reads mapping to both 3`-region of *RREB1* exon 8 (**B**) and to 5`-region of *MRTFB* exon 11 (**C**).

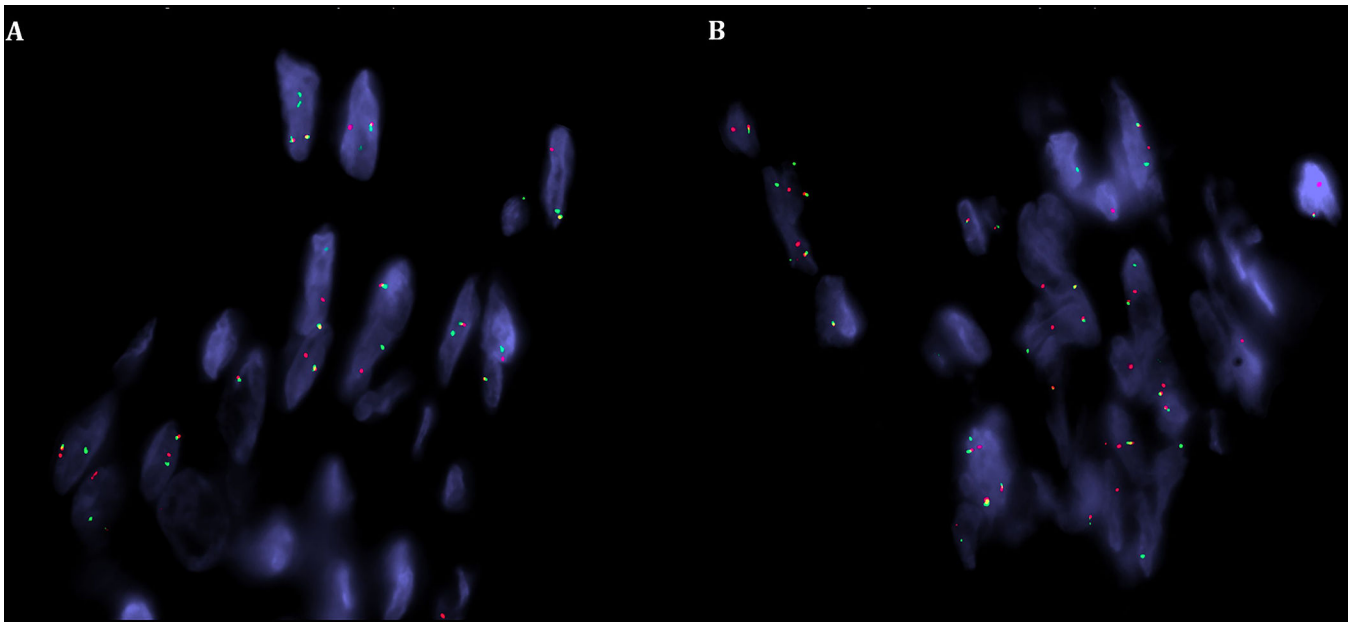

FIGURE 9.

FISH analysis revealed a break-apart signal for both *RREB1* (**A**) and *MRTFB* (**B**) (red, centromeric; green, telomeric) in keeping with balanced gene rearrangements.

Table 1:

Clinicopathological features of previously reported and current *RREB1::MRTFB* fusion positive extra-glossal neoplasms.

No	Case/ reference	Age/sex	Site	Size cm	Treatment	Outcome (duration)
1	Siegfried et al (2018) [13]	53/M	Retro-/parapharyngeal	3.5	Surgery + CRT	NED (10 mo)
2	Makise et al (2020) [14]	25/F	Neck/ superior mediastinum left	5.6	Surgery (piece-by-piece)	NED (27 mo)
3	Makise et al (2020) [14]	73/F	Superior mediastinum left	4.3	Surgery (piece-by-piece)	NED (18 mo)
4	Bubola et al (2020) [15]	37/F	Body of mandible right	3	Surgery	NA
5	Mechtersheimer et al (2021) [16]	73/F	Posterior middle nasal turbinate right	3.5	Surgery	NA
6	Current Case 1	61/M	Inguinal/proximal thigh left	8	Surgery	NED (17 mo)
7	Current Case 2	36/F	Presacral region	20	Surgery	Lost to follow-up
8	Current Case 3	28/F	Jaw (follicular cyst?)	NA	Surgery	Lost to follow-up
9	Current Case 4	28/M	Parapharyngeal space	6	Surgery	NED (5 mo)
10	Current Case 5	18/M	Posterior nasopharyngeal wall	3.3	Surgery	Very recent case

CRT=chemoradiotherapy; mo=months; NA=not available; NED=no evidence of disease.

Table 2:

Immunohistochemical and molecular findings in *RREB1::MRTFB* fusion positive extra-glossal neoplasms

No	Case/reference	Reported as	Histology patterns	Mitoses/10 hpfs	Positive IHC	Negative IHC	Fusion findings
1	Siegfried et al, 2018 [13]	Biphenotypic sarcoma	Monomorphic spindle cells fibrosarcoma-like	4	SMA, S100, desmin, myogenin	h-caldesmon, SOX10, EMA, p63, MUC4, AE1/AE3, CD34, STAT6, MDM2	*RREB1* exon 8/ *MRTFB* exon 11
2	Makise et al, 2020 [14]	Unclassified/extra-glossal EMCMT	Round > > spindle	<1	S100, GFAP, SMA, EMA, AE1/3, ER	Desmin, myogenin, SOX10, HMB45, MUC4, STAT6, CD34, BCOR, NKX2–2	*RREB1* exon 8/ *MRTFB* exon 11
3	Makise et al, 2020 [14]	Unclassified/extra-glossal EMCMT	Spindle >> round > myxoid	<1	S100, GFAP, SMA, EMA, AE1/3, pan-TRK, ER	AE1/AE3, desmin, myogenin, CD34, STAT-6, MUC4, SOX10, GLUT1, claudin-1, MDM2, DOG1, SSTR2a, ALK	*RREB1* exon 8/ *MRTFB* exon 11
4	Bubola et al (2020) [15]	EMCMT	EMCMT	0	SMA, S100, CD56, desmin, GFAP	SOX10, keratin (AE1/ AE3), chromogranin, calponin	*RREB1* exon 8/ *MRTFB* exon 11
5	Mechtersheimer et al, 2021 [16]	Biphenotypic sarcoma	Monomorphic spindle cells fibrosarcoma-like	1	SMA, S100, EMA, CD34	Desmin, myogenin, GFAP, STAT6, AE1/AE3	*RREB1* exon 8/ *MRTFB* exon 11
6	Current Case 1	Unclassified fibromyxoid neoplasm	Fibromyxoid, perineurioma-like whorls	5	CD34, EMA (F+), claudin1 (F+)	Pankeratin, STAT6, SMA, desmin, GLUT1, S100, SOX10, GFAP, ERG, MUC4, INI1 retained	*RREB1* exon 8/ *MRTFB* exon 11
7	Current Case 2	Unclassified fibromyxoid neoplasm	Fibromyxoid, chondromyxoid lobules	0	S100, CD68, EMA (F+)	Pankeratin, Brachyury, Claudin1, GFAP, MUC4, CD34, SOX10. INI1 retained	*RREB1* exon 8/ *MRTFB* exon 11
8	Current Case 3	Chondromyxoid sinonasal hamartoma	Chondromyxoid hamartoma-like	0	S100, CD56 (focal), SATB2 (wk.)	Pankeratin, ERG, ALK, Brachyury, MUC4, Pan-Trk, SSTR2A, Desmin, MDM2	*RREB1* exon 8/ *MRTFB* exon 11
9	Current Case 4	Unclassified spindle and round cell neoplasm	Monomorphic spindle and round cell, highly cellular	2	Synaptophysin, GFAP, CD56, patchy CD99 and PAX8	MUC4, NUT, Pan-TRK, STAT6, SS18 and ALK, EMA, p63, CK19, TLE1, S100, SMA, SOX10, CD34, CK34BetaE12, desmin, myogenin, Myo-D1, WT1, Chromogranin-A, Calcitonin, TTF1	*RREB1* exon 8/ *MRTFB* exon 11
10	Current Case 5	Low-grade mesenchymal neoplasm with rhabdomyoblastic differentiation and RREB::MRTFB fusion, not RMS	Monomorphic ovoid and round cells	1	MyoD1, desmin (focal), myogenin (focal)	GFAP, S100, betacatenin, CD34, CD117, CD3, CD19, CD45	*RREB1* exon 8/ *MRTFB* exon 11

EMCMT=ectomesenchymal chondromyxoid tumor; F=focal; IHC=immunohistochemistry; hpf=high power field; RMS=rhabdomyosarcoma.

Table 3:

Clinicopathological features of nasal chondromesenchymal hamartoma-like tumors tested in this study

No	Age (years)/sex	Site	Size cm	Positive IHC	Negative IHC	RNA sequencing	*DICER1* status	Signs of DICER1 syndrome
1	14/M	Ethmoid/maxillary left	7 (in aggregate)	S100, CD34	SOX10, ALK, betacatenin, ERG, SATB2, desmin, pankeratin, myogenin, EMA, GFAP, SMA	No fusion	No *DICER1* mutations	No
2 *	28/F	Jaw region 21–23 (follicular cyst?)	NA	S100, CD56 (focal), SATB2 (wk.)	Pankeratin, ERG, ALK, Brachyury, MUC4, Pan-Trk, SSTR2A, Desmin, MDM2	*RREB1::MTRFB*	No *DICER1* mutations	No
3	04/F	Nasal left	6	S100, SATB2 (wk.)	-	No fusion	No *DICER1* mutations	No

* Case 3 of the current study (ref. Table 1 and 2). wk.=weak staining.